9th International Congress of the Serbian Society of Mechanics
July 5-7, 2023, Vrnjačka Banja, Serbia

DEVELOPMENT OF A HYBRID FIXED-WING VTOL UNMANNED AERIAL VEHICLE

Radoslav D. Radulović[1], Milica P. Milić[1]

[1] Faculty of Mechanical Engineering,
The University of Belgrade, Kraljice Marije 16, 11120 Belgrade 35
e-mail: rradulovic@mas.bg.ac.rs, mmilic@mas.bg.ac.rs.

Abstract

As the use of unmanned aerial vehicles (UAV) in the world has expanded, the market needs for the development of multi-role unmanned systems are increasing. These unmanned systems tend to largely find their constant and irreplaceable role in many industries. The development of such systems is a complex process, which, among other things, must include detailed structural, static and dynamic calculations and testing. The UAV presented in this paper is a hybrid powered aircraft with vertical take-off and landing (VTOL) with a composite structure and an innovative hybrid propulsion with a starter-generator system. VTOL gives an advantage in the exploitation of the aircraft itself, because it does not require special ground conditions or space for take-off and landing. The starter and generator system enables a smaller amount of fixed mass, such as batteries, while the structure made of composite materials enables a smaller mass and the desired characteristics of strength, resistance to corrosion and fatigue. This paper present development review process of the latest technology in terms of the concept of system and subsystem operation, as well as financially favorable and high-quality construction.

Key words: Composite materials, Hybrid propulsion, VTOL UAV, development.

1. Introduction

In the recent years, the development and production of unmanned aerial vehicles (UAVs) are in expansion. UAVs exists in a various size and with wide ranges of performances, starting from micro-UAVs to the large UAVs categorized on the basis of take-off masses and overall dimensions and capability to long range flight. We can also categorize them by type of propulsion: electric, hybrid, jet propulsion, etc. So far, the most massive application of unmanned aerial vehicles has been shown in military and recreational purposes. Although prototypes are emerging for applications in other industries, such as transportation or performing operations which are potentially dangerous for humans etc. The most widespread type of UAVs is the multi-rotor, due to its simplicity of control, maneuverability and ability for vertical take-off and landing (VTOL). The main disadvantage of electric powered aircraft is energy consumption during cruise which results in relatively short operational time. Usually, fixed-wing UAVs provide much larger energy efficiency during cruise, but they require runways for take-off and landing and they do not have the possibility of VTOL configuration. Taking into account advantages of both types, the solution is to have a hybrid configuration, with VTOL abilities like multi-rotor aircrafts and energy efficiency during cruise like fixed-wing UAVs. This hybrid configuration can be obtained by integration of multiple rotors to the fixed-wing UAVs.

In recent years, electric propulsion of aircraft has attracted a lot of attention among researchers and innovators. Through research and testing, the main defect in the use of the electric propulsion was determined, namely specific density of batteries energy, which are applied as energy source in electric propulsion, is much lower than of kerosene, up to 60. On the other side, main benefits of the electric propulsion are: clean energy, low noise level, low mass of electric motors, without pollution caused by engine operation[1]. According to the latest research, the electric propulsion should become a real competitor to the conventional propulsion in the next ten years. New research increasingly leads to an increase in the specific density of batteries energy, as well as the use of ultra capacitors.

This paper presents an overview of the conceptual prototype solution of a hybrid unmanned aerial vehicle. This UAV is a VTOL configuration. It further says that it takes off and lands vertically with the help of four electric motors in a quadcopter configuration. This enables the aircraft to take off and land on any terrain. After reaching a certain height, the drive switches to the fifth engine, which is a piston engine, and the aircraft continues cruising with that engine. While the piston engine is running, the batteries are charged via a generator, specially developed and adapted to this system to use the power of the piston engine as energy to charge the batteries. The transition to hybrid propulsion is a modern technology that greatly contributes to the improvement of the autonomy of unmanned systems [2].

2. Requirements for the development of an unmanned aerial vehicle

Requirements for the development of this unmanned aerial vehicle primarily included propulsion and the method of exploitation. The aircraft should have the ability to take off and land vertically, so a VTOL configuration and the ability to take off and land conventionally. The structure should be composite and ensure the most optimal ratio of mass and strength of the structure. Transition to a piston engine and flight autonomy of up to 5 hours, with a payload of 25 kg. Mission of UAV is offensive UAV or for target positioning and irradiation.

General characteristics are:

Payload	25 kg
Gross Weight	87 kg
Fifth Engine	Piston Engine Twin Spark
Engine Power	14.5 kW
Minimal speed	70 km/h
Cruise speed	150 km/h
Maximum speed	200 km/h
Lift to drag ratio	13
Maximal vertical speed	7 m/s
Wing area	2.2 m^2
Wingspan	4.6 m
Aspect Ratio	9.62

Table 1. General characteristics of UAV

Table 1 shows the general characteristics fulfilled by the development of this unmanned aerial vehicle. The profile of the mission that the UAV fulfills can be described in several steps:

1. Vertical take-off and vertical climbing up to 1000m height with velocity of 4 m/s to 7m/s in quad-copter mode.

2. Transition from vertical to horizontal flight. This includes the electric start of the piston engine, the descent into horizontal flight and the shutdown of the electric engine.
3. Cruise and loitering with velocity of 120 km/h.
4. Transition from horizontal flight to hovering.
5. Hovering. Duration of hovering depends on the current charge of the batteries, which are charging for the duration of the horizontal flight via a generator, specially developed and adapted to this system.
6. Transition from hovering to horizontal flight.
7. Cruise to final destination.
8. Transition from horizontal flight to vertical flight. Reverse the procedure described in procedure 2.
9. Vertical landing with velocity of 4 m/s in quad-copter mode.

All requirements were taken into account when choosing the optimal methods for the development of this UAV.

3. Dimensioning of lifting surfaces

3.1. Wing geometry

The airfoil NASA/LANGLEY LS(1)-0417 (GA(W)-1) was chosen for the wing. The airfoil data are given in table 2. The maximum lift coefficient depending on the Reynolds number is given in table 3. These data were obtained on the basis of experimental research.

Maximum thickness	17%
Zero lift angle	-4.4°
Lift coefficient at zero angle of attack	0.52

Table 2. Basic information about the airfoil.

MRe	$c_{L\max}$
0.37	1.35
0.51	1.39
0.67	1.43
1.9	1.65

Table 3. Maximum airfoil lift coefficient depending on the Reynolds number.

The data given in Table 3 are graphically shown in Figure 1 and approximated by the following polynomial of the third degree:

$$c_{L\max} = 0.04436\mathrm{MRe}^3 - 0.1878\mathrm{MRe}^2 + 0.425\mathrm{MRe} + 1.216$$

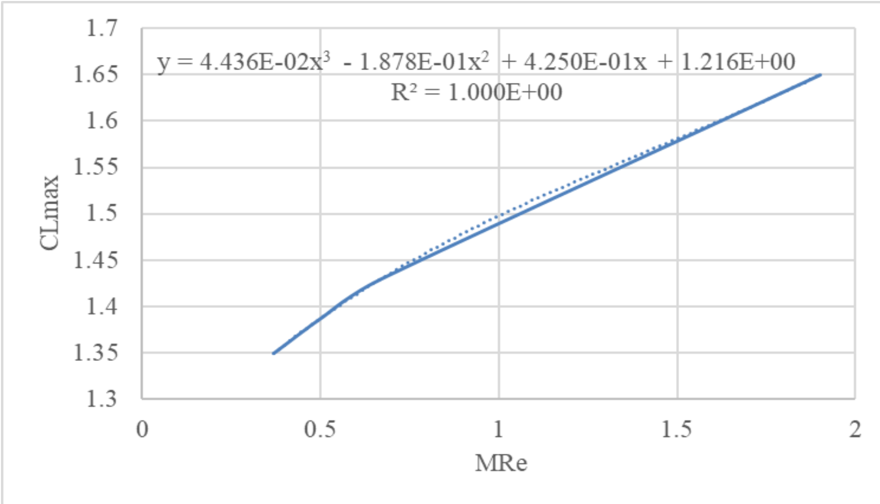

Fig. 1 Maximum drag coefficient of the airfoil depending on the Reynolds number

For the cruise mode of the aircraft, the Reynolds number 1MRe was estimated, so that the following maximum lift coefficient is obtained: $c_{L\max} = 1.5$.

The wing area is determined based on two criteria. The first criterion is cruising speed. The wing loading for cruise mode is obtained as follows:

$$\left(\frac{W}{S}\right)_{\mathrm{cr}} = \frac{1}{2g}\rho V_{\mathrm{cr}}^2 \sqrt{\pi A e C_{\mathrm{D0}}} = 54.078\,\mathrm{kg/m^2} \tag{1}$$

where A it represents the slenderness of the wing, for which the value is taken as 10, e is the Oswald factor, for which the value is taken as 0.8, while C_{D0} represents the coefficient of resistance of the aircraft at the angle of zero lift, for which the value is taken as 0.03. The second criterion is based on the speed of the overrun flight. The wing loading for this flight mode is:

$$\left(\frac{W}{S}\right)_{\mathrm{stall}} = \frac{1}{2g}\rho V_{\min}^2 C_{L\max} = 42.194\,\mathrm{kg/m^2} \tag{2}$$

where $C_{L\max}$ represents the maximum lift coefficient of the wing, which is taken to be 90% of the maximum airfoil lift: $C_{L\max} = 0.9 c_{L\max} = 1.35$. The authoritative value of the wing load for its dimensioning is the smaller value, which is obtained for the swept flight mode. For that mode, the following wing area is obtained: 2.062m^2.

3.2 Tail geometry

An inverted V tail is adopted. NACA0012 was taken for the airfoil of the tail surfaces. When calculating classic tail configurations, the horizontal and vertical are calculated separately, based on the geometric characteristics of the wings, the growth of the aerodynamic centers of the tails and wings, and adopted volume coefficients. For V and inverse V tails, the areas of the fictitious horizontal and vertical tails are calculated first. In theory, the area and angle of the V dihedral and the inverse V tail are obtained as follows:

$$S_{\mathrm{Tail}} = \sqrt{S_{\mathrm{H}}^2 + S_{\mathrm{V}}^2}\ ,\ \Gamma_{\mathrm{Tail}} = \arctan\frac{S_{\mathrm{V}}}{S_{\mathrm{H}}} \tag{3}$$

However, it is recommended that the area of these tail configurations be larger than theoretical, so the area and angle of the V dihedral and the inverse V tail are obtained as follows:

$$S_{\mathrm{Tail}} = S_{\mathrm{H}} + S_{\mathrm{V}}\,,\ \Gamma_{\mathrm{Tail}} = \arctan\sqrt{\frac{S_{\mathrm{V}}}{S_{\mathrm{H}}}} \tag{4}$$

Table 4 shows the adopted parameters for sizing tail surfaces.

The distance between the aerodynamic centers of the wings and the tail	$L = 2\mathrm{m}$
Tail constriction	$\lambda_{\mathrm{Tail}} = \frac{2}{3}$
Volumetric coefficient of the horizontal tail	$n_{\mathrm{H}} = 0.74$
Volumetric coefficient of the vertical tail	$n_V = 0.05$

Table 4. Parameters for dimensioning tail surfaces.

The horizontal and vertical tail surfaces are obtained as follows:

$S_{\mathrm{H}} = \frac{c_{\mathrm{H}} c_{\mathrm{MAC}} S}{L} = 0.3955\mathrm{m}^2$, $S_{\mathrm{V}} = \frac{c_{\mathrm{V}} b S}{L} = 0.2444\mathrm{m}^2$,

Where $c_{\mathrm{MAC}} = \frac{c_{\mathrm{MACi}} S_{\mathrm{i}} + c_{\mathrm{MACo}} S_{\mathrm{o}}}{S} = 0.503\mathrm{m}$ is the length of the aerodynamic chord of the wing, $b = 4.6\mathrm{m}$ wingspan and S=2.062m^2 wing area.

So, we get the area of the inverse V tail, as well as the angle of the dihedral:

$S_{\mathrm{Tail}} = 0.6399\mathrm{m}^2$, $\Gamma_{\mathrm{Tail}} = 38^{\mathrm{o}}$.

After dimensioning the lifting surfaces, a 3D model of the UAV was created and is shown in Fig.2.

Fig. 2. The 3D model of the VTOL UAV.

4. Aerodynamic calculation of finesse and polar in cruise regime

One of the most important phases of development is the aerodynamic calculation, after sizing the aerodynamic surfaces. The preliminary analytical aerodynamic calculation used in this paper shows that the UAV meets the performance of existing UAVs of that category, weighing up to 90 kg. The preliminary calculation was performed in accordance with the procedures described in the literature. [3,4,5,6].

4.1. Operating flight condition

In accordance with the intended mission of this UAV. Nominal flight altitudes are on the order of 500–1000 m. This calculation is performed for 500 m of flight altitude. The data from the Standard Atmosphere at a height of 500m are: air density ρ=1.16727 kg/m^3, coefficient of kinematic viscosity ν=1.79579E-05 m^2/s. These data are necessary for the calculation of the drag profile in cruise regime.

4.2. Aerodynamic forces

The maximum finesse of the aircraft is shown by the polar

$$C_X = C_{X0} + \frac{C_Z^2}{\pi A e} = 0.04039 + 0.04297 C_Z^2 \qquad (5)$$

The lift, drag and finesse coefficients for cruise regime are:

$$C_{Zcr} = \frac{2mg}{\rho V_{cr}^2 S} = 0.5371, \quad C_{Xcr} = 0.05278, \quad F_{cr} = \frac{C_{Zcr}}{C_{Xcr}} = 10.1758, \qquad (6)$$

and the maximum finesse of the aircraft is shown by the polar are:

$$C_{Zcr} = \frac{2mg}{\rho V_{cr}^2 S} = 0.96943, \quad F_{cr} = \frac{C_{Zcr}}{C_{Xcr}} = 12.002. \qquad (7)$$

With reference to previous relations, wing aspect ratio $\lambda = 9.876$ and Oswald factor of efficiency $e = 0.75$ the total drag coefficient on the cruise mode is $C_{Xcr} = 0.05278$ respectively lift coefficient $C_{Zcr} = 0.5371$, cruise speed $V_{cr} = 120\text{km/h}$.
A graphical representation of the polar and finesse is in Fig. 3.

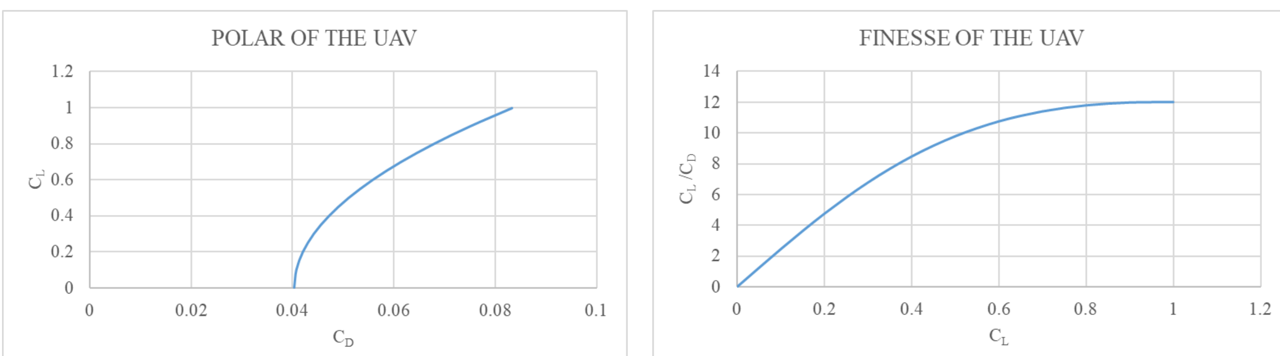

Fig. 3. Polar and Finesse of the UAV

If UAVs are categorized by weight, the expected finesse for this category of UAV and its performance is between $C_{Zcr} / C_{Xcr} = 7$ and $C_{Zcr} / C_{Xcr} = 13$. The refore, the preliminary calculation shows that the results are satisfactory.

5. Propulsion

5.1. Electric motors and batteries

Power for hovering and vertical climbing in quadcopter mode can be calculated using disc theory:

$$P_{\mathrm{h}} = \sum_{i=1}^{4} P_{\mathrm{h}i} = \sum_{i=1}^{4} T_i v_{\mathrm{h}i}, \quad P_{\mathrm{cl}} = \sum_{i=1}^{4} P_{\mathrm{cl}i} = \sum_{i=1}^{4} P_{\mathrm{h}i}\left[\frac{V_{\mathrm{cl}}}{2v_{\mathrm{h}i}} + \sqrt{\left(\frac{V_{\mathrm{cl}}}{2v_{\mathrm{h}i}}\right)^2 + 1}\right] \tag{8}$$

where T_i represents the thrust of the i-th propeller, V_{cl} is the climb speed in quadcopter mode, while $v_{\mathrm{h}i}$ represents the induced hover speed, which is calculated as follows:

$$v_{\mathrm{h}i} = \sqrt{\frac{T_i}{A_i}\frac{1}{2\rho}} = \sqrt{\frac{D_{\mathrm{L}i}}{2\rho}} \tag{9}$$

where $D_{\mathrm{L}i} = \dfrac{T_i}{A_i}$ represents the disk load of the i-th propeller. The power required for vertical descent cannot be calculated using disk theory for low speeds, so this power will be assumed to be equal to the power required for hovering. The required power of the i-th engine for hovering and vertical climbing is:

$$P_{\mathrm{eng\_h}i} = \frac{P_{\mathrm{h}i}}{\eta_{\mathrm{p}i}} = \frac{T_i v_{\mathrm{h}i}}{\eta_{\mathrm{p}i}}, \quad P_{\mathrm{eng\_cl}i} = \frac{P_{\mathrm{cl}i}}{\eta_{\mathrm{p}i}} = \frac{P_{\mathrm{h}i}}{\eta_{\mathrm{p}i}}\left[\frac{V_{\mathrm{cl}}}{2v_{\mathrm{h}i}} + \sqrt{\left(\frac{V_{\mathrm{cl}}}{2v_{\mathrm{h}i}}\right)^2 + 1}\right] \tag{10}$$

where $\eta_{\mathrm{p}i}$ represents the degree of utility of the i-th propeller.

The battery power required for hovering and vertical climbing is calculated as follows:

$$\begin{aligned} P_{\mathrm{bat\_h}} &= \sum_{i=1}^{4} \frac{P_{\mathrm{h}i}}{\eta_{\mathrm{p}i}\eta_{\mathrm{eng}i}\eta_{\mathrm{esc}i}\eta_{\mathrm{c}i}} = \sum_{i=1}^{4} \frac{T_i v_{\mathrm{h}i}}{\eta_{\mathrm{p}i}\eta_{\mathrm{eng}i}\eta_{\mathrm{esc}i}\eta_{\mathrm{c}i}}, \\ P_{\mathrm{bat\_cl}} &= \sum_{i=1}^{4} \frac{P_{\mathrm{cl}i}}{\eta_{\mathrm{p}i}\eta_{\mathrm{eng}i}\eta_{\mathrm{esc}i}\eta_{\mathrm{c}i}} = \sum_{i=1}^{4} \frac{P_{\mathrm{h}i}}{\eta_{\mathrm{p}i}\eta_{\mathrm{eng}i}\eta_{\mathrm{esc}i}\eta_{\mathrm{c}i}}\left[\frac{V_{\mathrm{cl}}}{2v_{\mathrm{h}i}} + \sqrt{\left(\frac{V_{\mathrm{cl}}}{2v_{\mathrm{h}i}}\right)^2 + 1}\right] \end{aligned} \tag{11}$$

The energy consumed by the hovering and vertical climbing battery is:

$$E_{\mathrm{bat\_h}} = P_{\mathrm{bat\_h}} t_{\mathrm{h}}, \quad E_{\mathrm{bat\_cl}} = P_{\mathrm{bat\_cl}} t_{\mathrm{cl}} \tag{12}$$

where t_{h} and t_{cl} represent the hovering and vertical climbing times, respectively [7].

Assuming that the finesse in horizontal flight is around 10, the disc loading for two-bladed propeller is $D_L = 268\mathrm{N/m^2}$, Table 5 presents the required energy from batteries for each segment of flight.

Energy from batteries	Vertical take-off and climbing	Hovering
(kW)	16	14.7

Table 5. Required energy from batteries for each segment of flight.

In accordance with the needs of the system, electric motors were chosen. With one engine, a maximum thrust of 303 N can be achieved, while the maximum power is 7.125kW. The maximum voltage that can be achieved with batteries is 53.9 V. The selected electric motors are the most efficient in this case and meet the needs of the project. The relationship between power and thrust is shown in Fig.4.

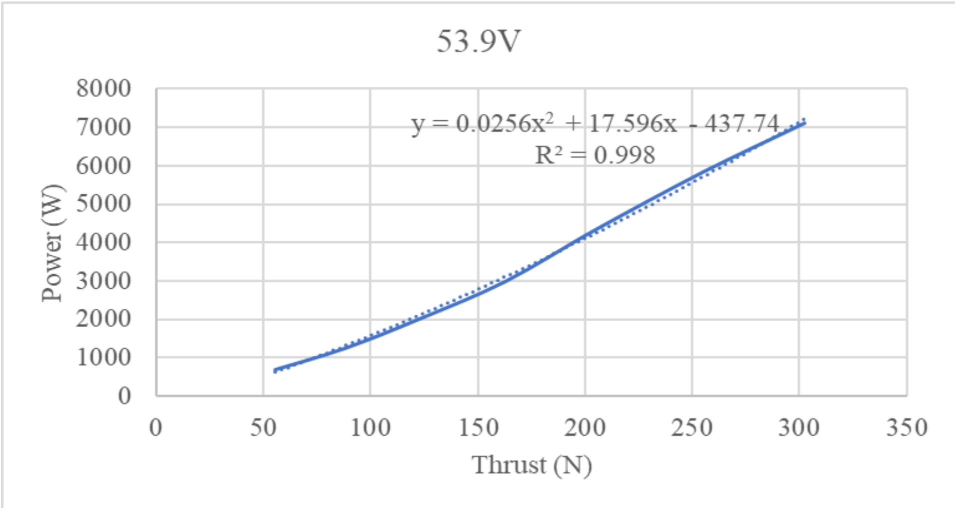

Fig. 4. The ratio of required power and thrust for vertical flight**.**

5.2. Calculation of the propulsion unit for horizontal flight

Aerodynamic drag in cruise mode is calculated as follows:

$$R_{X\mathrm{cr}} = \frac{1}{2}\rho V_{\mathrm{cr}}^2 S C_{X\mathrm{cr}} \tag{13}$$

Respectively,

$$R_{X\mathrm{cr}} = \frac{mg}{F_{\mathrm{cr}}} \tag{14}$$

The required thrust is equal to the aerodynamic drag force:

$$T_{\mathrm{cr}} = R_{X\mathrm{cr}} = \frac{1}{2}\rho V_{\mathrm{cr}}^2 S C_{X\mathrm{cr}} = \frac{mg}{F_{\mathrm{cr}}} = 49.4\mathrm{N} \tag{15}$$

The power of propulsion unit required for cruise mode is:

$$P_{\mathrm{cr}} = \frac{T_{\mathrm{cr}} V_{\mathrm{cr}}}{\eta_{\mathrm{p}}} = 2.195\mathrm{kW} \tag{16}$$

Where η_{p} represents the degree of utility of the propeller whose preliminary value is $\eta_{\mathrm{p}} = 0.75$.

5.3. Required power and thrust at maximum speed in horizontal flight

As with cruise regime, the thrust and required power at maximum speed in horizontal flight can be determined. Thrust is:

$$T_{\max} = R_{X\max} = \frac{1}{2}\rho V_{\max}^2 S C_{X\max} = \frac{mg}{F_{\max}} = 100.98\mathrm{N} \tag{17}$$

The power of propulsion unit required for cruise mode is:

$$P_{\max} = \frac{T_{\max} V_{\max}}{\eta_{\mathrm{p}}} = 7.48\mathrm{kW} \tag{18}$$

Based on the maximum speed of the aircraft, the required power of the propulsion group can be determined based on statistical parameters [4]:

$$\frac{P\left[\mathrm{hp}\right]}{W_0\left[\mathrm{lb}\right]} = aV_{\max}^{C}\left[\mathrm{ml/h}\right] \tag{19}$$

Where the parameters a and C are determined based on the ratio of power and mass of the aircraft. In the available literature [4], parameters can be find by category.

Based on the categorization from the literature, it can be seen that there is no clear classification of the aircraft that is the subject of the calculation. Therefore, two cases will be considered: "Homebuilt-composite" and "General aviation - single engine". Converting the mass of the aircraft and the maximum speed into the appropriate units of measurement, the following powers of the propulsion unit are obtained:

- first case: $P = 7.09\mathrm{kW}$
- second case: $P = 7.868\mathrm{kW}$

Based on the obtained results, it can be seen that the obtained values are very close to the value obtained by analytical calculation.

5.4. Power and thrust required for climbing in airplane mode

Thrust and power required for climb in airplane mode are obtained as follows:

$$T_{\mathrm{cl}} = \frac{1}{2}\rho V^2 C_X S + mg\frac{v_{\mathrm{cl}}}{V} \tag{20}$$

$$P_{\mathrm{cl}} = \frac{\frac{1}{2}\rho V^3 C_X S + mgv_{\mathrm{cl}}}{\eta_{\mathrm{p}}} \tag{21}$$

Thrust and required power were analyzed for multiple aircraft speeds in airplane mode and climb speed, to establish the highest values.

Results for speed of 120 km/h are shown in Table 6.

V[km/h]	v_{cl}[m/s]	T_{cl}[N]	P_{cl}[kW]
120	1	69.704	3.098
	2	90.306	4.0136
	3	110.907	4.929
	4	131.508	5.845
	5	152.109	6.76
	6	172.71	7.676

Table 6 Power and thrust required for climbing

5.5. Thrust and required power for a proper turn

The thrust required for a proper turn is calculated as follows:

$$T_{\mathrm{st}} = \frac{1}{2}\rho V^2 C_X S + \frac{n^2 m^2 g^2}{\frac{1}{2}\rho V^2 S\pi Ae} \tag{22}$$

Where n is the load coefficient. Assuming that the load factor is 3, and that the turn is performed at cruising speed, the following thrust value is obtained:

$T_{\mathrm{st}} = 184.655\mathrm{N}$

The required power of the power unit is:

$$P_{\mathrm{st}} = \frac{T_{\mathrm{st}} V_{\mathrm{cr}}}{\eta_{\mathrm{P}}} = 8.207\mathrm{kW}$$

Based on the previous power calculation, a piston engine with a maximum power of 13.2kW was selected. This engine was tested with several different propellers and accordingly the 28/12 propeller was chosen.

6. Conclusions

Development of fixed-wing VTOL UAV is still in rising phase. The corresponding aerodynamic configuration's improvement, design optimization of structure, flight control theory improvement and development and energy management technology still need to be improved. The research of fixed-wing VTOL UAV will become an important direction of aircraft's development.

This paper presents a preliminary calculation for the initial phases of the UAV development. As this is an early stage of the project, there remains the possibility of more detailed analysis, e.g. numerical calculation, testing and validation. Sometimes it is necessary to develop models for establishing the calculation, production and validation methodology, due to the deficiency of literature. Experience also plays an important role in such development projects. Also this paper presents the requirements that were met during the development of this multi role system. In addition, the basic parts of the preliminary conceptual design are presented.

Future work should include the integration of all subsystems and systems. Independent testing of piston engine and starter-generator and autopilot systems.

ORCID
Radoslav D. Radulovic https://orcid.org/0000-0002-9345-919X
Milica P. Milic https://orcid.org/0000-0003-4505-6086

Acknowledgements The authors would like to express their gratitude to EDePro company for research work on the project ALECS multirole system.

References

[1] Hepperle M., *Electric flight-potential and limitations*, Energy Efficient Technologies and Concepts of Operation, 22-24 October 2012, Lisbon, Portugal, 2012

[2] Ozdemir U., Aktas Y.,O., Vuruskan A., Dereli Y., Tarhan A.,F., Demirbag K., Erdem A., Kalaycioglu G.,D., Ozkol I., Inalhan G., *Design of a commercial hybrid VTOL UAV system*, Journal of Intelligent and Robotic Systems, Vol. 74, 371-393, 2014.

[3] Sadraey, M.H.: Unmanned aircraft design. A review of fundamentals, Morgan & Claypool Publishers, 2017

[4] Reymer, D.,P., Aircraft Design: a ConceptualApproach, Third edition, AIAA, Reston, Virginia, USA, 1999.

[5] Roskam J., *Airplane Design, Part VI: Preliminary Calculation of Aerodynamic, Thrust and Power Characteristic*, Roskam Aviation and Engineering Corporation, Ottawa, Kansas, USA, 1987.

[6] Roskam J., *Airplane Design, Part VII: Determination of Stability, Control and Performance Characteristic: FAR and Military Requirements*, Roskam Aviation and Engineering Corporation, Ottawa, Kansas, USA, 1988.

[7] Gloudemans, J., Davis, P., Gelhausen, P.: A rapid geometry modelerfor conceptual aircraft. In: 34th Aerospace Sciences Meeting and Exhibit. AIAA, Reston,1996.